Integral Action NMPC for Tight Maneuvers of Articulated Vehicles

You, Sixiong; Greiff, Marcus; Quirynen, Rien; Ran, Shuangxuan; Wang, Yebin; Berntorp, Karl; Dai, Ran; Di Cairano, Stefano

TR2023-058 June 01, 2023

Abstract

We propose an integral action nonlinear model predictive controller (NMPC) for trajectory tracking of an articulated vehicle with an uncertain hitching offset. The controller is intended for complex parking maneuvers including forward and backward movement with tight specifications on the lateral positional tracking error of the trailer. In order to assess performance with uncertain hitching offsets, disturbances, and sensor noise, we conduct extensive hardware-in-the-loop simulations using a dSPACE Scalexio unit. With high-grade sensing, we demonstrate that the closed-loop control system achieves a lateral tracking error of < 3 [cm] in expectation, and an absolute terminal error of < 15 [cm] with high probability $p > 0.97$. The proposed integral action is shown to be essential in achieving this performance, and the efficacy of the proposed NMPC is evaluated by comparison to alternative MPCs.

American Control Conference (ACC) 2023

Integral Action NMPC for Tight Maneuvers of Articulated Vehicles

Sixiong You[1], Marcus Greiff[2], Rien Quirynen[2], Shuangxuan Ran[3], Yebin Wang[2], Karl Berntorp[2], Ran Dai[1], and Stefano Di Cairano[2]

***Abstract*— We propose an integral action nonlinear model predictive controller (NMPC) for trajectory tracking of an articulated vehicle with an uncertain hitching offset. The controller is intended for complex parking maneuvers including forward and backward movement with tight specifications on the lateral positional tracking error of the trailer. In order to assess performance with uncertain hitching offsets, disturbances, and sensor noise, we conduct extensive hardware-in-the-loop simulations using a dSPACE Scalexio unit. With high-grade sensing, we demonstrate that the closed-loop control system achieves a lateral tracking error of < 3 [cm] in expectation, and an absolute terminal error of < 15 [cm] with high probability $p > 0.97$. The proposed integral action is shown to be essential in achieving this performance, and the efficacy of the proposed NMPC is evaluated by comparison to alternative MPCs.**

I. INTRODUCTION

Autonomous vehicle technologies have long attracted great interest within the research community due to their great potential in improving fuel efficiency, driving safety and traffic flows [1]. In particular, autonomous control of the semi-trailer articulated vehicles have the potential to revolutionize the transportation and logistics sectors [2]. However, safe tracking control of such vehicles becomes difficult when considering complex parking and docking maneuvers with realistic disturbances and modeling errors, and such maneuvers are critical to a fully autonomous solution. Consequently, we propose controllers for precise parking with a tractor towing a single trailer with an uncertain hitching offset (see Fig. 1), as this offset is often not known exactly.

There exists a large body of work that can be leveraged in such a control system design [3]. Specifically, the *standard* n-trailer (SNT) considered in this paper (see Fig. 1) is known to be differentially flat, even when there is a non-zero hitching offset [3]. The considered system differs from the *general* n-trailer (GNT) in [4], which does not satisfy the same properties. The SNT model admits an exact feedback linearization [5], [6], which results in powerful nonlinear feedback laws that can be combined with linear control synthesis techniques (see, e.g., [7]). However, such designs are sensitive to modeling errors, and cannot easily incorporate state constraints necessary to ensure safety.

Based on these practical considerations, many prior works focus on path tracking control of articulated vehicles using model predictive control (MPC). When restricted to *forward motion* (cruise control), both linear and nonlinear MPC (NMPC) have been proposed for path tracking control of the S1T and G1T-systems [8]–[10]. Alternative methods of path tracking control with *forward and backward* motions have been considered for special paths (motion primitives), such as linear segments and circular trajectories. Backward motion implies significant challenges, as any modeling errors are greatly amplified through a chain of unstable systems.

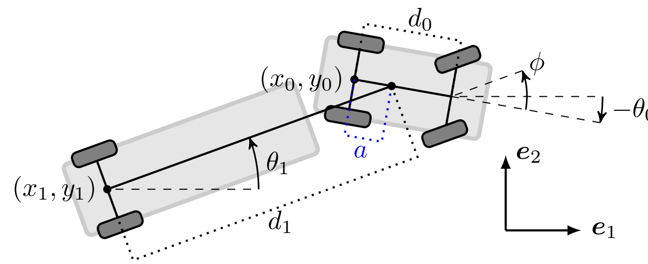

Fig. 1. Geometry of the considered S1T-system with a hitching offset, a.

When considering trajectory tracking of *arbitrary dynamically feasible motions*, both MPC and NMPC have been shown to achieve good tracking performance [11]–[15]. The work in [11] describes a distributed NMPC scheme to reduce computations, and [14] proposes a gradient-based approach tailored for real-time execution. In the present paper, we will compare such gradient-based solvers to a proposed sequential quadratic programming (SQP) approach, and demonstrate real-time execution with the `PRESAS` solver [16].

A. Contributions

A subset of the cited works yield good performance for tracking of arbitrary dynamically feasible paths with both forward and backward motion, but the impact of modeling errors such as a (i) constant steering angle bias, (ii) an incorrect hitching offset and (iii) actuator dynamics are generally not considered. We propose an NMPC with integral action (iNMPC), where an integral tracking error is introduced in the iNMPC prediction model. Our contributions are twofold:

- An integral action NMPC utilizing SQP with `PRESAS`, and a tailored cost function that is shown to be essential for good tracking and robustness when reversing the tractor trailer system in practice. This is necessary for autonomous loading operations at a docking bay.
- Quantitative numerical results from hardware-in-the-loop simulations carried out on the dSPACE Scalexio unit [17], analyzing the controller design with realistic modeling errors in Monte–Carlo (MC) simulations.

[1]School of Aeronautic and Astronautics, Purdue University, IN, 47907, USA. Emails: {you84,randai}@purdue.edu. [2]Mitsubishi Electric Research Labs (MERL), 02139 Cambridge, MA, USA. Email to corresponding author: greiff@merl.com. [3]University of Michigan. Ann Arbor, MI, 48109, USA. Email: ssran@umich.edu.

B. Notation

Vectors are written $\boldsymbol{x} \in \mathbb{R}^n$ with x_i denoting the i^{th} element of $\boldsymbol{x}$, and matrices are indicated in bold font as $\boldsymbol{X}$. Here, $\boldsymbol{x} \sim \mathcal{N}(\boldsymbol{\mu}, \boldsymbol{\Sigma})$ indicates that $\boldsymbol{x}$ is Gaussian distributed with mean $\boldsymbol{\mu}$ and covariance $\boldsymbol{\Sigma}$, and $\boldsymbol{x} \sim \mathcal{U}(I)$ indicates that $\boldsymbol{x}$ is uniformly distributed over an interval I. We let $p(\boldsymbol{y}|\boldsymbol{x})$ be a conditional probability density function of $\boldsymbol{y}$ given $\boldsymbol{x}$. Additionally, $\|\boldsymbol{x}\|_2^2 = \boldsymbol{x}^\top \boldsymbol{x}$ and we let $\|\boldsymbol{x}\|_{\boldsymbol{A}}^2 = \boldsymbol{x}^\top \boldsymbol{A}\boldsymbol{x}$. Throughout the paper, the notation $\Sigma : \boldsymbol{x}_{k+1} = \boldsymbol{f}_{\boldsymbol{\theta}}(\boldsymbol{x}_k, \boldsymbol{u}_k)$ refers to a discrete-time dynamical system that is to be controlled. The system Σ_r denotes a *reference* system where signals are super-indexed by $(\cdot)^r$, Σ_s denotes a system that is used in the *synthesis* of a controller, and Σ_η is an *integral* system. These systems generally do not have the same state-space. We write sequences of a signal $\boldsymbol{x}_k$ over an interval $k \in [a, b] \subseteq \mathbb{N}_{>0}$ as $\boldsymbol{x}_{a:b} = \{\boldsymbol{x}_a, \ldots, \boldsymbol{x}_b\} = \{\boldsymbol{x}_k\}_{k=a}^b$.

II. MODELING

The considered semi-trailer system is modeled as a standard 1-trailer, with wheelbase $d_1 > 0$ [m] and a hitching offset $a \in [0, d_0]$ [m], configured on $(x_0, y_0, \theta_0, \theta_1) \in \mathbb{R}^2 \times (\mathsf{S}^1)^2$ (see Fig. 1). Here, (x_0, y_0) [m] is the center position of the tractor's rear axle in the global frame, and θ_0 [rad] and θ_1 [rad] are heading angles of tractor and trailer, respectively. We also consider first order actuator dynamics to account for the low-level controllers of the semi-trailer,

$$\dot{x}_0 = v\cos(\theta_0), \tag{1a}$$
$$\dot{y}_0 = v\sin(\theta_0), \tag{1b}$$
$$\dot{\theta}_0 = \tfrac{v}{d_0}\tan(\phi + \phi_b), \tag{1c}$$
$$\dot{\theta}_1 = \tfrac{v}{d_1}\sin(\theta_0 - \theta_1) + \tfrac{av}{d_0 d_1}\tan(\phi + \phi_b)\cos(\theta_0 - \theta_1), \tag{1d}$$
$$\dot{v} = \tfrac{1}{\tau_1}(v_d - v), \tag{1e}$$
$$\dot{\phi} = \tfrac{1}{\tau_2}(\phi_d - \phi), \tag{1f}$$

where v and v_d [m/s] refer to the actual and desired longitudinal velocity of the tractor, ϕ and ϕ_d [rad/s] refer to the actual and desired steering angle of tractor. The actuator dynamics are defined by time constants $\tau_i > 0$ [s]. In addition, we include a constant unknown steering angle bias of ϕ_b [rad].

In (1), the desired velocity v_d and desired ϕ_d are control commands that are required by the low-level control-by-wire system. The resulting model has a state vector $\boldsymbol{x} = (x_0, y_0, \theta_0, \theta_1, v, \phi) \in \mathbb{R}^4 \times (\mathsf{S}^1)^2$, a control vector $\boldsymbol{u} = (v_d, \phi_d) \in \mathbb{R}^2$, and model parameters $\boldsymbol{\theta} = (d_0, d_1, a, \tau_0, \tau_1, \phi_b) \in \mathbb{R}^5_{>0} \times \mathbb{R}$. The continuous-time system in (1) is discretized using a standard 4^{th}-order Runge-Kutta method at a constant time-step of h [s], and written as

$$\Sigma: \ \boldsymbol{x}_{k+1} = \boldsymbol{f}_{\boldsymbol{\theta}}(\boldsymbol{x}_k, \boldsymbol{u}_k), \tag{2}$$

with $t_k = hk \geq 0$, $k \in \mathbb{N}_{\geq 0}$, often dropping $\boldsymbol{\theta}$ for brevity.

Remark 1 *The continuous-time system in* (1) *is differentially flat [3], but requires one additional degree of smoothness over the classical S1T system due to the first-order actuator dynamics. As such, it may be controlled effectively using feedback linearization and related planning techniques. However, the flat output space becomes less useful for planning when $a > 0$, and the system becomes uncontrollable as $a \to d_0$ for reverse motions $v_d < 0, v < 0$.*

Remark 2 *While the system* (1) *is open-loop stable in forward motion, $v_d > 0, v > 0$, it is unstable in backward motion, and any modeling error of the hitching offset acts as a disturbance on the unstable modes of the system.*

When evaluating the controllers, we do not assume perfect knowledge of the states, but rather consider a stochastic measurement model defined with a Gaussian likelihood

$$\boldsymbol{y}_k \sim p(\boldsymbol{y}_k|\boldsymbol{x}_k) = \mathcal{N}(\boldsymbol{x}_k, \operatorname{diag}(\sigma_{x_0}^2, \sigma_{y_0}^2, \sigma_{\theta_0}^2, \sigma_{\theta_1}^2, \sigma_v^2, \sigma_\phi^2)).$$

Similarly, the initial conditions of the controlled system in the ith simulation is sampled from a Gaussian distribution

$$\boldsymbol{x}_0^{(i)} \sim p(\boldsymbol{x}_0) = \mathcal{N}(\boldsymbol{x}_0^r, \operatorname{diag}(\sigma_{0,1}^2, \sigma_{0,2}^2, \sigma_{0,3}^2, \sigma_{0,4}^2, \sigma_{0,5}^2, \sigma_{0,6}^2)),$$

with parameters given in Appendix . In the simulation studies, we assume that the reference system, Σ_r, and the system used for controller synthesis, Σ_s, are parameterized in the same *nominal* model parameters. However, the system that is controlled, Σ, is parameterized by $\boldsymbol{\theta}^{(i)} \sim p(\boldsymbol{\theta})$ which for the i^{th} simulation is sampled from a distribution over the model parameters (refer to the appendix for details).

III. LINEAR MODEL PREDICTIVE CONTROL

In this section, we introduce the standard linear MPC and the sub-optimal time-distributed MPC (TDMPC) [18] for linear time-varying dynamical systems of the form

$$\boldsymbol{x}_{k+1} = \boldsymbol{A}_k \boldsymbol{x}_k + \boldsymbol{B}_k \boldsymbol{u}_k. \tag{3}$$

These controllers will serve as benchmarks for the proposed iNMPC in the forthcoming simulation studies.

A. The Optimal Control Problem

Let $\boldsymbol{x}_k^r$ and $\boldsymbol{u}_k^r$ denote the reference state and control signal trajectories governed by a reference system Σ_r, and let $\boldsymbol{\xi}_k = \boldsymbol{y}_k - \boldsymbol{x}_k^r$, $\boldsymbol{\nu}_k = \boldsymbol{u}_k - \boldsymbol{u}_k^r$. These errors are considered over a prediction horizon of length N, and for simplicity, we let $\bar{k} = k + N$. To minimize the tracking error, the linear MPC determines the control action by solving an associated optimal control problem (OCP), here defined following [18],

$$\min_{\boldsymbol{\xi}_{k:\bar{k}}, \boldsymbol{\nu}_{k:\bar{k}-1}} \|\boldsymbol{\xi}_{\bar{k}}\|_{\boldsymbol{P}}^2 + \sum_{\tau=k}^{\bar{k}-1} \|\boldsymbol{\xi}_\tau\|_{\boldsymbol{Q}}^2 + \|\boldsymbol{\nu}_\tau\|_{\boldsymbol{R}}^2, \tag{4a}$$

subject to

$$\boldsymbol{\xi}_k = \boldsymbol{y}_k - \boldsymbol{x}_k^r, \tag{4b}$$
$$\boldsymbol{\xi}_{\tau+1} = \boldsymbol{A}_\tau \boldsymbol{\xi}_\tau + \boldsymbol{B}_\tau \boldsymbol{\nu}_\tau, \qquad \tau = k, \ldots, \bar{k}-1, \tag{4c}$$
$$\boldsymbol{\nu}_{\min} \leq \boldsymbol{\nu}_\tau \leq \boldsymbol{\nu}_{\max}, \qquad \tau = k, \ldots, \bar{k}-1, \tag{4d}$$

where $\boldsymbol{Q} \succeq \boldsymbol{0}$, $\boldsymbol{R} \succ \boldsymbol{0}$, and $\boldsymbol{P} \succeq \boldsymbol{0}$ are weight matrices defining the quadratic forms in the tracking errors. Upon solving (4) at a time k for $\boldsymbol{\nu}_{k:\bar{k}-1}^\star$, the system is actuated with the first element in this sequence, letting $\boldsymbol{u}_k = \boldsymbol{u}_k^r + \boldsymbol{\nu}_k^\star$. This procedure is repeated on every time step (see Fig. 2).

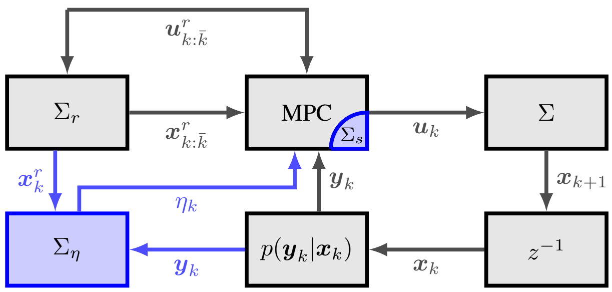

Fig. 2. Block diagram of a controlled system, Σ, driven along the trajectory of a reference system, Σ_r, by an MPC controller. The blue color indicates items that differ between a standard MPC and the proposed iNMPC. Specifically, the difference is in the computation of the integral term η in Σ_η, and the modification of Σ_s used in the MPC synthesis.

B. Linearizations

As the articulated vehicle system in (2) is nonlinear, we consider a first-order expansion of the dynamics about the reference trajectory. At the time step k, this results in

$$\boldsymbol{\xi}_{k+1} = \left[\frac{\partial \boldsymbol{f}_{\boldsymbol{\theta}}(\boldsymbol{x},\boldsymbol{u})}{\partial \boldsymbol{x}} \quad \frac{\partial \boldsymbol{f}_{\boldsymbol{\theta}}(\boldsymbol{x},\boldsymbol{u})}{\partial \boldsymbol{u}}\right]\Bigg|_{(\boldsymbol{x},\boldsymbol{u})=(\boldsymbol{x}^r_k,\boldsymbol{u}^r_k)} \begin{bmatrix}\boldsymbol{\xi}_k\\ \boldsymbol{\nu}_k\end{bmatrix} + o\left(\left\|\begin{bmatrix}\boldsymbol{\xi}_k\\ \boldsymbol{\nu}_k\end{bmatrix}\right\|^2\right)$$
$$\approx \boldsymbol{A}(\boldsymbol{x}^r_k,\boldsymbol{u}^r_k)\boldsymbol{\xi}_k + \boldsymbol{B}(\boldsymbol{x}^r_k,\boldsymbol{u}^r_k)\boldsymbol{\nu}_k, \tag{5}$$

where the first constant term in the Taylor series vanishes due to the linearization being about the reference trajectory. For simplicity, we let $\boldsymbol{A}_k \triangleq \boldsymbol{A}(\boldsymbol{x}^r_k,\boldsymbol{u}^r_k)$, $\boldsymbol{B}_k \triangleq \boldsymbol{B}(\boldsymbol{x}^r_k,\boldsymbol{u}^r_k)$, and generate function handles for the Jacobians in (5) using the `CasADi` software [19], which is a free and open source framework for automatic differentiation and code generation.

C. Solving the Optimal Control Problem

To solve the OCP formulated in (4), we first write the problem in a condensed form. Following [18, Section 3], let

$$\min_{\bar{\boldsymbol{\nu}}_k\in\mathcal{U}} \left\|\begin{bmatrix}\bar{\boldsymbol{\nu}}_k\\ \boldsymbol{\xi}_k\end{bmatrix}\right\|^2_{\boldsymbol{M}_k}, \qquad \boldsymbol{M}_k = \begin{bmatrix}\boldsymbol{H}_k & \boldsymbol{G}_k\\ \boldsymbol{G}_k^\top & \boldsymbol{W}_k\end{bmatrix}, \tag{6}$$

where $\bar{\boldsymbol{\nu}}_k^\top = (\boldsymbol{\nu}_k^\top,\dots,\boldsymbol{\nu}_{\bar{k}-1}^\top)$, and $\mathcal{U}$ denotes a set representing the constraints in (4d). Here, the components of $\boldsymbol{M}_k$ are defined as in [18, Appendix A], but with time-varying $\boldsymbol{A}_{k:\bar{k}-1}, \boldsymbol{B}_{k:\bar{k}-1}$. The problem in (6) can be solved to appropriate numerical tolerances using off-the-shelf methods. Here, formulating (6) using a linearization about the reference with respect to an `RK4` discretization of the continuous ODE in (1), and solving the OCP with Matlab's `quadprog` is referred to as a linear MPC (LMPC). We also consider the sub-optimal time-distributed approach in [18], using the accelerated projected gradient method (APGM) defined in [18, Algorithm 2], run for a number of iterations on each time-step that exceeds the theoretical limit that guarantees stability in a linear setting [18, Corollary 4]. Solving the standard MPC problem in this way is referred to as TDMPC.

IV. INTEGRAL ACTION NMPC WITH SQP

Considering the steering angle bias, the hitching offset and the nonlinear kinematics of the system in (1), we introduce the iNMPC to satisfy the requirements of high accuracy on the terminal lateral position and heading angle of trailer for complex parking and docking maneuvers [20], [21].

A. Lateral Integral Tracking Error

To achieve good tracking during challenging reversing maneuvers, the trailer's lateral positional integral tracking error is computed in the reference frame of the trailer, and introduced as a new state variable, η, with dynamics,

$$\dot{\eta} = \cos(\theta^r_1)(x_1 - x^r_1) - \sin(\theta^r_1)(y_1 - y^r_1), \tag{7}$$

where θ^r_1 is the desired heading angle of trailer, and x_1 [m] and y_1 [m] denote the Cartesian position of the center of trailer's rear axle in the global frame (see Fig. 1),

$$\begin{aligned} x_1 &= x_0 - \cos(\theta_1)d_1 + \cos(\theta_0)a, \\ y_1 &= y_0 - \sin(\theta_1)d_1 + \sin(\theta_0)a. \end{aligned} \tag{8}$$

With $\eta(0) = 0$, the integral error can be evaluated approximately at a time $t = hk$ in the state trajectory $\boldsymbol{x}_{0:k}$ and the reference trajectory $\boldsymbol{x}^r_{0:k}$. With a slight abuse of notation,

$$\Sigma_\eta: \ \eta_{k+1} = \int_0^{h(k+1)} \dot{\eta}(\sigma)\mathrm{d}\sigma \approx \eta_k + h\dot{\eta}_k(\boldsymbol{x}_k,\boldsymbol{x}^r_k). \tag{9}$$

In practice, this error is computed recursively in the measured signals $\boldsymbol{y}_{0:k}$, that is using $\dot{\eta}_k(\boldsymbol{y}_k,\boldsymbol{x}^r_k)$ as illustrated in Fig. 2. In the model used for the synthesis of the iNMPC, the original state vector in the controlled system (1) is complemented with the integral state, resulting in a new state vector $\bar{\boldsymbol{x}} = (x_0, y_0, \theta_0, \theta_1, v, \phi, \eta) \in \mathbb{R}^5 \times (\mathsf{S}^1)^2$. This system is once again discretized using an `RK4` scheme as in (2), yielding

$$\Sigma_s: \ \bar{\boldsymbol{x}}_{k+1} = \boldsymbol{f}^s_{\boldsymbol{\theta}}(\bar{\boldsymbol{x}}_k, \boldsymbol{u}_k). \tag{10}$$

B. Objective Function

To minimize tracking errors, a quadratic objective function is formulated over a prediction horizon of length $N \in \mathbb{N}_{>0}$. For convenience, we let $\bar{k} = k + N$. To start, a stage cost is expressed as quadratic forms in the tracking errors over the prediction horizon, defined by $\boldsymbol{Q} \succeq \boldsymbol{0}$ and $\boldsymbol{R} \succ \boldsymbol{0}$, and a terminal cost is expressed as a quadratic form in $\boldsymbol{P} \succeq \boldsymbol{0}$ at the terminal time $\bar{k}$. Furthermore, to generate smooth steering commands and permit constraints on the relative heading angles, an performance output vector is defined as $\boldsymbol{z} = (x_1, y_1, \dot{\eta}, \theta_0 - \theta_1, \dot{v}, \dot{\phi}) = \boldsymbol{g}(\bar{\boldsymbol{x}}, \boldsymbol{u})$, and the standard MPC cost function in (4a) is complemented by quadratic forms in $\boldsymbol{z}_k$ defined by $\boldsymbol{T} \succeq \boldsymbol{0}$. We introduce a set of non-negative slack variables $s_{k:\bar{k}}$ to implement soft constraints on $\bar{\boldsymbol{x}}_{k:\bar{k}}$ and $\boldsymbol{z}_{k:\bar{k}}$, ensuring feasibility of the resulting optimization problem. These slack variables are weighted by a parameter

$\rho > 0$ included in the cost, resulting in an objective function

$$J(\bar{\boldsymbol{x}}_{k:\bar{k}}, \boldsymbol{u}_{k:\bar{k}-1}, s_{k:\bar{k}}) = \frac{1}{2}\sum_{\tau=k}^{\bar{k}-1} \|\boldsymbol{z}_\tau - \boldsymbol{z}_\tau^r\|_{\boldsymbol{T}}^2 + \frac{1}{2}\sum_{\tau=k}^{\bar{k}} \rho s_\tau + \frac{1}{2}\sum_{\tau=k}^{\bar{k}-1}(\|\bar{\boldsymbol{x}}_\tau - \bar{\boldsymbol{x}}_\tau^r\|_{\boldsymbol{Q}}^2 + \|\boldsymbol{u}_\tau - \boldsymbol{u}_\tau^r\|_{\boldsymbol{R}}^2) + \frac{1}{2}\|\bar{\boldsymbol{x}}_{\bar{k}} - \bar{\boldsymbol{x}}_{\bar{k}}^r\|_{\boldsymbol{P}}^2. \tag{11}$$

C. The Optimal Control Problem

With the objective in (11) and given some $\boldsymbol{\theta}$, the discrete-time optimal control problem for the iNMPC reads as

$$\min_{\boldsymbol{u}_{k:\bar{k}-1}, \bar{\boldsymbol{x}}_{k:\bar{k}}, s_{k:\bar{k}}} J(\bar{\boldsymbol{x}}_{k:\bar{k}}, \boldsymbol{u}_{k:\bar{k}-1}, s_{k:\bar{k}}), \tag{12a}$$

subject to

$$\bar{\boldsymbol{x}}_k = (\boldsymbol{y}_k^\top, \eta_k)^\top, \tag{12b}$$
$$\bar{\boldsymbol{x}}_{\tau+1} = \boldsymbol{f}_{\boldsymbol{\theta}}^s(\bar{\boldsymbol{x}}_\tau, \boldsymbol{u}_\tau), \quad \tau = k, \ldots, \bar{k}-1, \tag{12c}$$
$$\boldsymbol{z}_\tau = \boldsymbol{g}(\bar{\boldsymbol{x}}_\tau, \boldsymbol{u}_\tau), \quad \tau = k, \ldots, \bar{k}-1 \tag{12d}$$
$$\boldsymbol{u}_{\min} \leq \boldsymbol{u}_\tau \leq \boldsymbol{u}_{\max}, \quad \tau = k, \ldots, \bar{k}-1, \tag{12e}$$
$$\boldsymbol{z}_{\min} - s_\tau \leq \boldsymbol{z}_\tau \leq \boldsymbol{z}_{\max} + s_\tau, \quad \tau = k, \ldots, \bar{k}-1, \tag{12f}$$
$$\bar{\boldsymbol{x}}_{\min} - s_\tau \leq \bar{\boldsymbol{x}}_\tau \leq \bar{\boldsymbol{x}}_{\max} + s_\tau, \quad \tau = k, \ldots, \bar{k}, \tag{12g}$$
$$s_\tau \geq 0, \quad \tau = k, \ldots, \bar{k}, \tag{12h}$$

which aims to find the optimal sequence of steering actions $\boldsymbol{u}_{k:\bar{k}-1}$ that minimizes the objective function while satisfying the system dynamics, control signal constraints and state constraints. Here, (12e) includes inequality constraints on the steering angle and velocity, the state constraints (12g) and (12f) include inequality constraints on the relative heading angle of trailer and tractor, steering rate and acceleration. In addition, the slack variables $s_\tau \geq 0$ are used in the soft state constraints (12g) and (12f), guaranteeing feasibility of the constrained optimal control problem (12) at every time step. As in Section III, the output of the NMPC controller is the first element in the sequence of control signals $\boldsymbol{u}_{k:\bar{k}-1}^\star$ when solving the OCP in (12) on each time step k.

D. Solving the Optimal Control Problem

We solve the nonlinear program in (12) within the sampling period of $h = 50$ [ms] by a tailored implementation of sequential quadratic programming (SQP) known as the real-time iterations (RTI) scheme [22]. The RTI algorithm performs a single SQP iteration per control time step, and uses a continuation-based warm starting of the state and control trajectories from one time step k to the next $k+1$. The nonlinear functions and their first order derivatives are evaluated efficiently using C code generation in `CasADi` [19]. We use the QP solver `PRESAS` [16], which applies block-structured factorization techniques with low-rank updates to preconditioning of an iterative solver within a primal active-set algorithm. In combination with the `CasADi` generated C code, this results in an efficient NMPC solver that is suitable for embedded systems. In case of time delays, e.g., due to the vehicle network communication and/or actuator interface, a time delay compensation can be used [23].

TABLE I

COMPARISON OF THE TERMINAL ERRORS WITH THE TWO NMPCS IN 10^3 MC-RUNS WITH **FORWARD** MOTION ALONG A **STRAIGHT PATH**

Error	Unit	iNMPC		Regular NMPC	
		Mean	2σ	*Mean*	2σ
$x_0 - x_0^r$	[m]	0.0001	0.021	0.0021	0.023
$y_0 - y_0^r$	[m]	0.0017	0.0308	0.0308	0.0357
$\lvert\dot{\eta}\rvert$	[m]	**0.0013**	0.0170	0.0170	0.0177

TABLE II

COMPARISON OF THE TERMINAL ERRORS WITH THE TWO NMPCS IN 10^3 MC-RUNS WITH **BACKWARD** MOTION ALONG A **STRAIGHT PATH**

Error	Unit	iNMPC		Regular NMPC	
		Mean	2σ	*Mean*	2σ
$x_0 - x_0^r$	[m]	-0.0002	0.0171	-0.0003	0.0276
$y_0 - y_0^r$	[m]	0.0003	0.0465	-0.1534	0.056
$\lvert\dot{\eta}\rvert$	[m]	**0.0001**	0.032	0.1534	0.055

V. NUMERICAL EXPERIMENTS

The results in this section are generated based on hardware-in-the-loop (HIL) simulations using a dSPACE Scalexio DS-6001 processor board [17]. The motion planner and controller are defined with the nominal parameters, but the parameters of the system and the initial tracking errors are uncertain, and sampled uniquely for each simulation (refer to the appendix). The statistics of the tracking errors are computed from a large number of Monte-Carlo (MC) simulations, and we are primarily interested in their value at the end of the maneuvers. We start by analyzing the effects of integral action in the NMPC for a simple straight path, followed by a comparison of the linear MPCs in Section III and the NMPCs in Section IV on a complex parking maneuver. Finally, we study the effects of hitching offsets on the tracking errors, as this is a critical parameter for the success of tight maneuvering in practice.

A. Forward and Backward Motion Along a Straight Path

To validate the proposed iNMPC method and highlight the importance of including integral action, we start by comparing a regular and integral action NMPCs when controlling the vehicle along the straight path. Inspired by [4], we define two different controllers for forward and backward motion, respectively. The intuition being that the forward controller should focus more on the tracking error of the tractor's states, while the backward controller should focus more on the tracking error of the trailer's states. The controller tuning is provided in the appendix, and the only difference between the NMPCs is that the integral state η is not considered in the regular NMPC. The time step of NMPC is $h = 0.05$ [s], and the prediction horizon is $N = 40$ steps.

A MC-study is conducted with 10^3 realizations of $\{\boldsymbol{\theta}^{(i)}, \boldsymbol{x}_0^{(i)}\}_{i=1}^{10^3}$, and the results are reported in Fig. 3 and Tables I–II. In Table I, we observe a small bias in the lateral tracking error (shaded in gray) primarily caused by

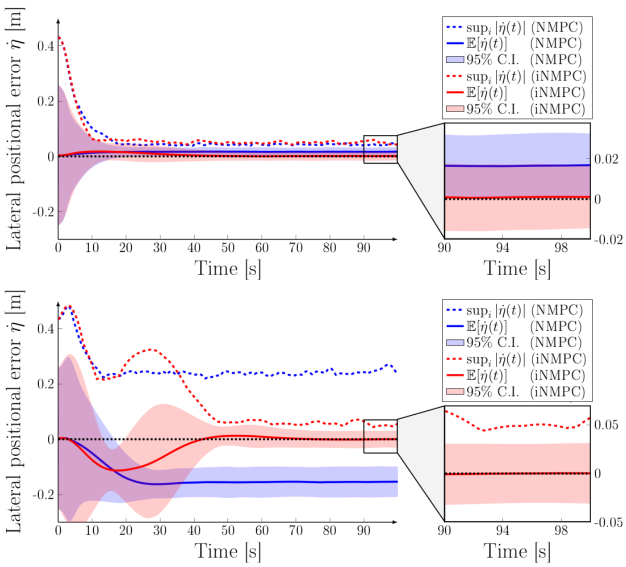

Fig. 3. Comparison of lateral positional tracking error, $\dot{\eta}$, with the regular NMPC (blue) and the iNMPC (red), with statistics from 10^3 MC-executions. The 2σ-interval is depicted along with the largest tracking error at every point in time over all of the realizations (dotted), with a zoom on the terminal errors. *Top*: Forward motion. *Bottom*: Backward motion.

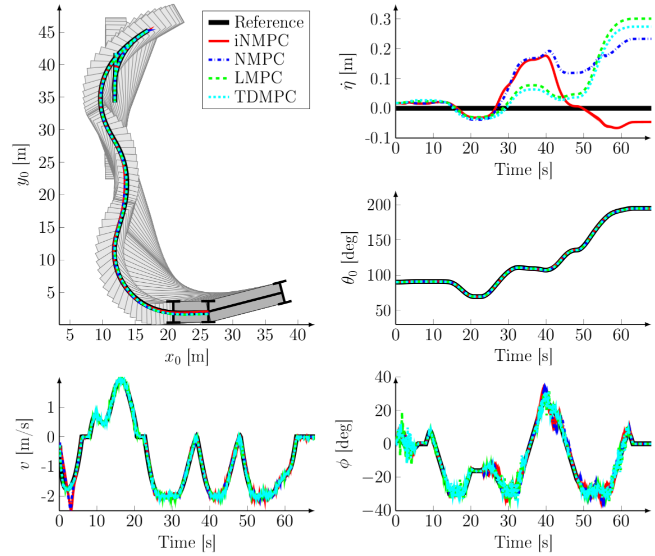

Fig. 4. One MC-simulation with the iNMPC (red), regular NMPC (blue), standard linear MPC (green) and TDMPC (cyan). *Top, left*: Configurations of the iNMPC response, and positional response $(x_0(t), y_0(t))$ with all considered controllers. The wheelbases are drawn for the terminal configuration. *Top, right*: The lateral positional tracking error. *Center, right*: The trailer heading angle. *Bottom, left*: Velocity. *Bottom, right*: Steering angle.

the steering angle bias. This error in the regular NMPC is tolerable, but becomes significantly smaller in the iNMPC when including integral action. For backward motion, the steering angle bias and modeling errors result in much larger tracking errors (see Table II). The inclusion of the integral tracking error greatly reduces the impact of such modeling errors, yielding near perfect tracking in expectation during backward motion with the iNMPC.

This is further illustrated in Fig. 3. Focusing on backward motion, we note that the iNMPC achieves a near perfect tracking (in expectation) after 40 [s], while the regular NMPC clearly exhibits a stationary tracking error. Furthermore, we note that for the given nominal parameter ranges, the 95% confidence interval of the terminal tracking error is in the range of 3 [cm] with the iNMPC. The probability of the regular NMPC achieving such low tracking errors is vanishingly small. Finally, when studying the worst tracking error reported at each time-step across all of the MC-runs, it is evident that there are outliers for some particularly problematic vehicle parameters that yield errors in the range of ≈ 5 [cm] in the iNMPC and ≈ 22 [cm] in the NMPC.

To summarize, the integral action in the proposed iNMPC greatly reduces the tracking errors in backward motion, which is necessary for tight parking maneuvers. In particular, the iNMPC is effective in dealing with the steering angle bias, hitching offsets, and other considered modeling errors. Next, we considering a more complex and realistic parking maneuver where small tracking errors are safety-critical.

B. Autonomous Parking and Docking Maneuver

We now consider a complex parking maneuver generated by a motion planning algorithm based on bi-directional A-search guided tree (BIAGT) [24]. As the success of the maneuver depends on the trailer's lateral positional error and heading error at the terminal time, these signals will be the focus of our comparison. We now include simulations with:

(i) The standard LMPC, implemented as in Section III;
(ii) The TDMPC in [18] as described in Section III;
(iii) The standard NMPC in Section IV, *omitting* η in Σ_s;
(iv) The iNMPC in Section IV, *including* η in Σ_s,

and present results from Matlab simulations and HIL simulations on Scalexio [17].[1] In contrast to the previous example, we make the simulation more realistic by including gear shifting dynamics, forcing the vehicle to stand still 1.5 [s] while shifting between forward and reverse gears. The velocity is constrained to $v(t) \in [0, 3]$ [m/s] and $v \in [-3, 0]$ [m/s] in forward and backward motion, respectively. Furthermore, as the parking maneuver is preceded by forward path following, we sample the initial tracking errors in accordance with the stationary tracking error distribution reported for the forward motion in Table I (see parameters in the appendix).

One of 10^3 MC-realizations is shown in Fig. 4, and the statistics of the simulation study are summarized in Table III. All of the considered controllers yield visibly good trajectory tracking in this particular realization. However, a closer inspection of the error statistics shows that the benchmark MPC approaches (i)–(iii) result in significant offsets in the trailer's lateral tracking error. For the specific maneuver considered in Fig. 4, the expected terminal lateral errors for the regular NMPC, linear MPC and TDMPC are 0.1672 [m], 0.1298 [m] and 0.1177 [m], respectively. Intuitively, an NMPC will do a better job at utilizing the nonlinear prediction model, and should yield better performance if we have the same parameterization of Σ_r and Σ. As there is a

[1]The NMPCs are implemented in Simulink, but the linear MPCs are simulated in Matlab. As such, the noise realizations differ in the MC runs.

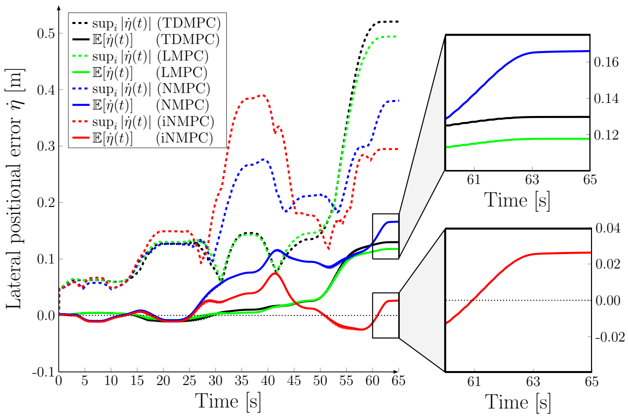

Fig. 5. Lateral positional tracking error, $\dot{\eta}$, with the iNMPC (red), regular NMPC (blue), LMPC (green) and TDMPC (yellow), summarizing the statistics from 10^3 MC-executions in terms of the mean error (full line) and the largest absolute error over all realizations (dotted).

TABLE III
COMPARISON OF THE TERMINAL ERRORS WITH THE FOUR CANDIDATE MPCS IN 10^3 MC-RUNS WITH A **COMPLEX PARKING MANEUVER**

Error	Unit	iNMPC		Regular NMPC	
		Mean	2σ	*Mean*	2σ
$x_0 - x_0^r$	[m]	0.0896	0.1082	0.1400	0.0435
$y_0 - y_0^r$	[m]	0.1843	0.2540	0.0347	0.2516
$\lvert\dot{\eta}\rvert$	[m]	**0.0274**	0.1310	0.1672	0.2263
Error	**Unit**	**Linear MPC**		**TDMPC**	
		Mean	2σ	*Mean*	2σ
$x_0 - x_0^r$	[m]	0.1650	0.0558	0.1627	0.0563
$y_0 - y_0^r$	[m]	-0.1004	0.2605	-0.0895	0.2595
$\lvert\dot{\eta}\rvert$	[m]	0.1298	0.2852	0.1177	0.2850

modeling mismatch, for this particular maneuver, the linear MPCs outperform the NMPC in expectation. However, the variance of the NMPCs terminal lateral positional tracking error is smaller than that of the linear MPCs. A such, the worst realizations in the linear MPC yields significantly larger errors than the NMPC.

In contrast to the benchmark controllers, the trailer's terminal lateral error of the iNMPC is 0.0274 [m]. Indeed, the MC results in Table III confirm this to be the case, with the iNMPC achieving an expected terminal lateral tracking error of < 3 [cm] and an absolute error of <15 [cm] with probability $p = 0.976$, despite the noise and disturbances added in the simulations. When studying Fig. 5, we observe a significant difference in the worst tracking error achieved over the MC-executions. This is in the range of 0.5 [m] with the LMPC and TDMPC. The iNMPC never exceeds 0.3 [m].

Finally, to demonstrate that the iNMPC implementation is real-time feasible, the computation times for solving the OCP in (12) on the Scalexio unit are provided in Fig. 6. These timings never exceed the limit of 50 [ms] when running the iNMPC at 20 [Hz] with a horizon length $N = 40$. Indeed, most computation times are well below this threshold, with an average computation time of < 4 [ms] per time-step.

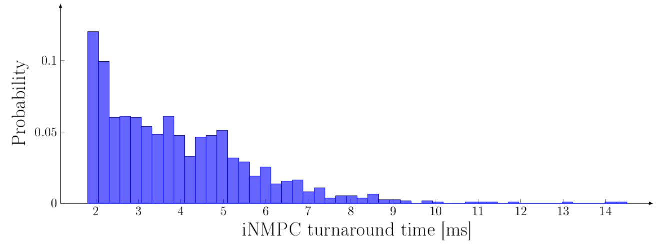

Fig. 6. Computation times per control time step of the iNMPC in Scalexio.

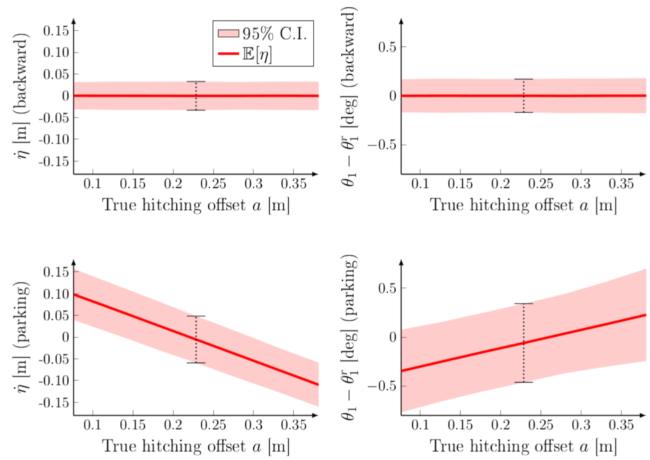

Fig. 7. The 95% confidence interval of the tracking error with the iNMPC as a function of the hitching offset in the controlled system, Σ, from 10^3 MC simulations. The dashed lines indicate the terminal errors when the hitching offset is known. *Top*: Backward motion. *Bottom*: Parking maneuver.

C. Robustness to Hitching Offsets

As mentioned in Remark 2 and demonstrated in Section V-A, modeling errors in the hitching offset have significant effects on the trailer's heading angle and lateral position, particularly in reverse motions. To study the robustness of the iNMPC to such modeling errors, the nominal offset of Σ_r and Σ_s is assumed to be 0.2286 [m], while the actual hitching offset of the simulation model, Σ, is varied from 0.076 [m] to 0.381 [m]. We reuse the backward motion along a straight path and parking maneuver in Section V-B. The simulation results are presented in Fig. 7, showing the 95% confidence interval of the terminal lateral positional and heading errors of the trailer as a function of the hitching offset.

For backward motions along a straight path, we find that the trailer's lateral error and heading error are constant as a function of the offset modeling error (top two subplots). Here, the iNMPC achieves perfect tracking in expectation. However, for the parking maneuver, the trailer's lateral error and heading error are approximately linear in the hitching offset (bottom two subplots). Here, we speculate that the maneuver is too short to completely suppress the effects of the hitching errors. As such, while the proposed iNMPC improves performance in expectation under an uncertain hitching offset with respect to the three benchmark MPCs (see Fig. 4), there is trade-off between performance and the hitching-offset uncertainty for complex parking maneuvers.

VI. CONCLUSIONS

We present an integral action NMPC to address the problem of steering angle biases and uncertain hitching offsets in complex articulated vehicle parking, involving both gear shifting dynamics and non-standard reference trajectories. In particular, we leverage `CasADi` and `PRESAS` to construct an SQP-based controller that directly minimizes the lateral positional integral tracking error. This approach was found to yield significant performance improvements over the three considered benchmark MPCs (the standard LMPC, the TDMPC, and the standard NMPC), especially when considering maneuvers that involve reversing. These conclusions were drawn from several MC studies with hardware-in-the-loop simulations, involving measurement noise, parameter errors, and realistic parking maneuvers generated by BI-AGT [24]. We found that the proposed iNMPC resulted in an expected terminal lateral tracking error of <3 [cm] for this maneuver, significantly better than the benchmark MPCs.

Future work will include running experiments to validate the integral action NMPC using a real articulated vehicle.

REFERENCES

[1] F. Duarte and C. Ratti, "The impact of autonomous vehicles on cities: A review," *Journal of Urban Tech.*, vol. 25, no. 4, pp. 3–18, 2018.

[2] C. Fritschy and S. Spinler, "The impact of autonomous trucks on business models in the automotive and logistics industry–a delphi-based scenario study," *Technological Forecasting and Social Change*, vol. 148, p. 119736, 2019.

[3] P. Rouchon, M. Fliess, J. Lévine, and P. Martin, "Flatness, motion planning and trailer systems," in *IEEE Conf. on Decision and Control*, 1993, pp. 2700–2705.

[4] C. Altafini, A. Speranzon, and B. Wahlberg, "A feedback control scheme for reversing a truck and trailer vehicle," *IEEE Trans. robotics and automation*, vol. 17, no. 6, pp. 915–922, 2001.

[5] M. Sampei, T. Tamura, T. Kobayashi, and N. Shibui, "Arbitrary path tracking control of articulated vehicles using nonlinear control theory," *IEEE Trans. Control Systems Tech.*, vol. 3, no. 1, pp. 125–131, 1995.

[6] P. Bolzern, R. M. DeSantis, A. Locatelli, and D. Masciocchi, "Path-tracking for articulated vehicles with off-axle hitching," *IEEE Trans. control systems technology*, vol. 6, no. 4, pp. 515–523, 1998.

[7] H. K. Khalil, "Nonlinear systems third edition," *Patience Hall*, 2002.

[8] E. Kayacan, W. Saeys, H. Ramon, C. Belta, and J. M. Peschel, "Experimental validation of linear and nonlinear MPC on an articulated unmanned ground vehicle," *IEEE/ASME Trans. Mechatronics*, vol. 23, no. 5, pp. 2023–2030, 2018.

[9] T. Xu, X. Ji, Y. Liu, and Y. Liu, "Differential drive based yaw stabilization using MPC for distributed-drive articulated heavy vehicle," *IEEE Access*, vol. 8, pp. 104 052–104 062, 2020.

[10] H. Sahin and O. Akalin, "Articulated vehicle lateral stability management via active rear-wheel steering of tractor using fuzzy logic and model predictive control." *SAE Int. Commercial Vehicles*, vol. 13, no. 2, pp. 115–129, 2020.

[11] E. Kayacan, E. Kayacan, H. Ramon, and W. Saeys, "Distributed nonlinear model predictive control of an autonomous tractor–trailer system," *Mechatronics*, vol. 24, no. 8, pp. 926–933, 2014.

[12] M. Abroshan, R. Hajiloo, E. Hashemi, and A. Khajepour, "Model predictive-based tractor-trailer stabilisation using differential braking with experimental verification," *Vehicle system dynamics*, vol. 59, no. 8, pp. 1190–1213, 2021.

[13] Z. Brock, J. Nelson, and R. L. Hatton, "A comparison of lateral dynamic models for tractor-trailer systems," in *IEEE Intell. Vehicles Symposium*, 2019, pp. 2052–2059.

[14] M. Lukassek, A. Völz, T. Szabo, and K. Graichen, "Model predictive path-following control for general n-trailer systems with an arbitrary guidance point," in *IEEE European Cont. Conf.*, 2021, pp. 1335–1340.

[15] O. Ljungqvist, D. Axehill, H. Pettersson, and J. Löfberg, "Estimation-aware model predictive path-following control for a general 2-trailer with a car-like tractor," *arXiv preprint arXiv:2002.10291*, 2020.

[16] R. Quirynen and S. Di Cairano, "PRESAS: Block-structured preconditioning of iterative solvers within a primal active-set method for fast model predictive control," *Optimal Control Applications and Methods*, vol. 41, no. 6, pp. 2282–2307, 2020.

[17] dSPACE, "Scalexio product page," Last accessed 8/3-22, dspace.com/en/inc/home/products/hw/simulator/scalexio.cfm.

[18] D. Liao-McPherson, T. Skibik, J. Leung, I. Kolmanovsky, and M. M. Nicotra, "An analysis of closed-loop stability for linear model predictive control based on time-distributed optimization," *IEEE Trans. Automatic Control*, vol. 67, no. 5, pp. 2618–2625, 2021.

[19] J. A. Andersson, J. Gillis, G. Horn, J. B. Rawlings, and M. Diehl, "CasADi: a software framework for nonlinear optimization and optimal control," *Math. Prog. Comp.*, vol. 11, no. 1, pp. 1–36, 2019.

[20] M. Morari and U. Maeder, "Nonlinear offset-free model predictive control," *Automatica*, vol. 48, no. 9, pp. 2059–2067, 2012.

[21] G. Pannocchia, "Offset-free tracking MPC: A tutorial review and comparison of different formulations," in *IEEE European control conf.*, 2015, pp. 527–532.

[22] S. Gros, M. Zanon, R. Quirynen, A. Bemporad, and M. Diehl, "From linear to nonlinear MPC: bridging the gap via the real-time iteration," *Int. Control*, vol. 93, no. 1, pp. 62–80, 2020.

[23] S. Di Cairano and I. V. Kolmanovsky, "Real-time optimization and model predictive control for aerospace and automotive applications," in *Amer. Control Conf.*, 2018, pp. 2392–2409.

[24] Y. Wang, "Improved a-search guided tree construction for kinodynamic planning," in *IEEE Int. conf. on Robotics and Automation*, 2019, pp. 5530–5536.

APPENDIX

The parameters in Table IV correspond to high-grade sensing and articulated semi-trailer with standard US dimensions.

TABLE IV

PARAMETERS USED IN THE QUANTITATIVE SIMULATION STUDIES.

Simulation parameter	Controlled system (Σ)	Nominal (Σ_r, Σ_s)	Unit	Description
$\sigma_{x_0}, \sigma_{y_0}$	0.05	–	m	Position noise
$\sigma_{\theta_0}, \sigma_{\theta_1}$	0.2	–	deg	Heading noise
σ_v	0.01	–	m/s	Velocity noise
σ_ϕ	0.1	–	deg/s	Steering rate noise
$\sigma_{0,1}, \sigma_{0,2}$	0.1	–	m	Position error (Sec. V-A)
$\sigma_{0,3}, \sigma_{0,4}$	0.4	–	deg	Heading error (Sec. V-A)
$\sigma_{0,5}$	0.02	–	m/s	Velocity error (Sec. V-A)
$\sigma_{0,6}$	0.2	–	deg/s	Steering error (Sec. V-A)
$\sigma_{0,1}, \sigma_{0,2}$	0.01	–	m	Position error (Sec. V-B)
$\sigma_{0,3}, \sigma_{0,4}$	0.05	–	deg	Heading error (Sec. V-B)
$\sigma_{0,5}$	0.01	–	m/s	Velocity error (Sec. V-B)
$\sigma_{0,6}$	0.025	–	deg/s	Steering error (Sec. V-B)
d_0	5.38	5.38	m	Wheel base (tractor)
d_1	11.73	11.73	m	Wheel base (trailer)
a	$\mathcal{U}$([0.08, 0.38])	0.229	m	Hitching offset
τ_0	$\mathcal{U}$([0.9,1.1])	0.1	s	Actuator time const.
τ_1	$\mathcal{U}$([0.9,1.1])	0.1	s	Actuator time const.
ϕ_b	1	0	deg	Steering angle bias

TABLE V

DIAGONAL ELEMENTS OF THE WEIGHT MATRICES OF THE NMPC COST.

Par.	Forward Motion	Backward Motion
$\boldsymbol{Q}$	$[10, 10, 5, 0.1, 0.5, 0.8, 1]$	$[0.2, 0.2, 0.1, 200, 0.5, 0.6, 1.5]$
$\boldsymbol{T}$	$[0.1, 0.1, 0.1, 1, 10, 1]$	$[5, 5, 8, 20, 5, 6]$
$\boldsymbol{P}$	$[10, 10, 5, 0.1, 0.5, 0.8, 1]$	$[0.2, 0.2, 0.1, 200, 0.5, 0.6, 1.5]$
$\boldsymbol{R}$	$[0.1, 0.1]$	$[0.1, 0.1]$
ρ	20	20
Var.	**Lower Bound $(\cdot)_{\min}$**	**Upper Bound $(\cdot)_{\max}$**
$\bar{\boldsymbol{x}}$	$[\star, \star, 0, 0, -3, -36, \star]$	$[\star, \star, 360, 360, 3, 36, \star]$
$\boldsymbol{u}$	[-3,-36]	[3,36]
$\boldsymbol{z}$	$[\star, \star, \star, -89, -5, 36, -15]$	$[\star, \star, \star, 89, 1, 36, 15]$